Title	Synthesis, Photo-, and Electrochemistry of Ruthenium Bis(bipyridine) Complexes Comprising a N-heterocyclic Carbene Ligand
Author(s)	Leigh, Vivienne; Ghattas, Wadih; Lalrempuia, Ralte; Müller-Bunz, Helge; Pryce, Mary T.; Albrecht, Martin
Publication date	2013-05-06
Publication information	Inorganic Chemistry, 52 (9): 5395-5402
Publisher	American Chemical Society
Item record/more information	http://hdl.handle.net/10197/6595
Publisher's statement	This document is the unedited author's version of a Submitted Work that was subsequently accepted for publication in Inorganic Chemistry, copyright © American Chemical Society after peer review. To access the final edited and published work, see http://pubs.acs.org/doi/abs/10.1021/ic400347r.
Publisher's version (DOI)	http://dx.doi.org/10.1021/ic400347r

Synthesis, Photo-, and Electrochemistry of Ruthenium Bis(bipyridine) Complexes Comprising a *N*-heterocyclic Carbene Ligand

Vivienne Leigh,[†] Wadih Ghattas,[†] Ralte Lalrempuia,[†] Helge Müller-Bunz,[†] Mary T. Pryce,[‡] and Martin Albrecht[†]*

† School of Chemistry & Chemical Biology, University College Dublin, Belfield, Dublin 4, Ireland

‡ School of Chemical Sciences, Dublin City University, Glasnevin, Dublin 9, Ireland

* martin.albrecht@ucd.ie; Fax: +353 17162501; Phone: +353 17162504.

ABSTRACT. Analogues of $[Ru(bpy)_3]^{2+}$ were prepared in which one pyridine ligand site is substituted by a N-heterocyclic carbene (NHC) ligand, *i.e.* either by an imidazolylidene with a variable wingtip group R (R = Me, **3a**; R = Et, **3b**; R = *i*Pr, **3c**), or by a benzimidazolylidene (Me wingtip group, **3d**) or by a 1,2,3-triazolylidene (Me wingtip group, **3e**). All complexes were characterized spectroscopically, photophysically, and electrochemically. An increase of the size of the wingtip groups from Me to Et or *i*Pr groups distorts the octahedral geometry (NMR spectroscopy) and curtails the reversibility of the ruthenium oxidation. NHC ligands with methyl wingtip groups display reversible ruthenium oxidation at a potential that reflects the donor properties of the NHC ligand (triazolylidene > imidazolylidene > benzimidazolylidene). The most attractive properties were measured for the triazolylidene ruthenium complex **3e**, featuring the smallest HOMO-LUMO gap in the series (2.41 eV), a slightly red-shifted absorption profile, and reasonable excited-state lifetime (188 ns) when compared to $[Ru(bpy)_3]^{2+}$. These features demonstrate the potential utility of triazolylidene ruthenium complexes as photosensitizers for

solar energy conversion.

Introduction

Efficient harnessing of solar energy as a renewable fuel intrinsically depends on efficient photosensitizers for the harvesting of light.[1] As an alternative to the vast range of organic photosensitizing materials,[2] metal complexes have become increasingly attractive as their excited state often induces facile charge separation and consequently the generation of an electrical circuit. Complexes of iridium,[3] copper,[4] platinum,[5] iron,[6] rhenium,[7] and osmium[8] have been used as sensitizers, though the most abundant systems are undoubtedly those derived from $[Ru(bpy)_3]^{2+}$.[9] In particular, these photoactive complexes have been used extensively and successfully in dye-sensitized solar cells (DSSCs).[10] Different approaches have been proposed to refine and improve the photoactivity of ruthenium, including for example the introduction of metallacyclic motifs.[11] Our interest in N-heterocyclic carbene (NHC) chemistry[12,13] and especially in their application for materials[14] prompted us to explore the potential utility of carbene ligands as substitutes for pyridine to enhance the photosensitising ability of $[Ru(bpy)_3]^{2+}$ analogues.[15] Specifically, the strong donor properties of NHCs[12] are expected to reduce the oxidation potential of the ruthenium center, which in turn should facilitate charge separation in the excited state, *ie* lowering the activation energy for the transition of Ru^{2+}* to $Ru^{3+} + e^-$.[16] Preliminary studies using picolyl-substituted NHC complexes suggest that the electrochemical response is indeed beneficially altered by the presence of a coordinating NHC ligand, though photophysical measurements revealed no emission.[17] Here we have refined our design to access useful excited states. Specifically, we have used pyridyl-substituted NHC ligands comprised of a direct bond between the pyridyl and the NHC ligands[15] rather than a $–CH_2–$ spacer as in the picolyl systems studied originally. This modification yields luminescent ruthenium(II) complexes. Variation in the NHC unit indicates that the properties of the metal center can be efficiently tailored.

Results and Discussion

Synthesis. A set of five pyridyl-carbene ruthenium complexes was prepared as depicted in Scheme 1. The synthetic strategy involved the preparation of chelating ruthenium *p*-cymene complexes via transmetalation followed by ligand substitution. Thus, the pyridyl-functionalized azolium salts **1a–e** were treated with silver oxide in either CH_3CN or CH_2Cl_2 in the absence of light to give the corresponding silver carbene complex,[18] which was not isolated but transmetalated in situ by filtering the reaction mixture directly into a solution of $[RuCl_2(p\text{-cymene})]_2$.[19] Complexes **2a–e** were obtained in moderate to good yields (46–70%) as air-stable orange solids. Ruthenation was confirmed by NMR spectroscopy and mass spectrometry. The most diagnostic feature is the loss of the acidic azolium proton, in the ^{1}H NMR spectra and the appearance of the diagnostic AB doublet between 5.70 and 6.40 ppm, which integrated for the four aryl protons of the cymene ligand. In the ^{13}C NMR spectra, the resonances for the ruthenium-bound carbenic carbons appeared in the typical 180(±5) ppm range for the imidazolylidene complexes, slightly below 200 ppm for the benzimidazolylidene complex **2d**, and at 174 ppm for **2e**.[19c] As noted for related carbene complexes with *i*Pr wingtip groups,[19] rotation about the N–C$_{i\text{Pr}}$ bond is slow on the NMR time scale and gives rise to two doublets in **2c** (δ_H = 1.72 and 1.40 ppm; δ_C 23.8 and 22.8 ppm).

Scheme 1

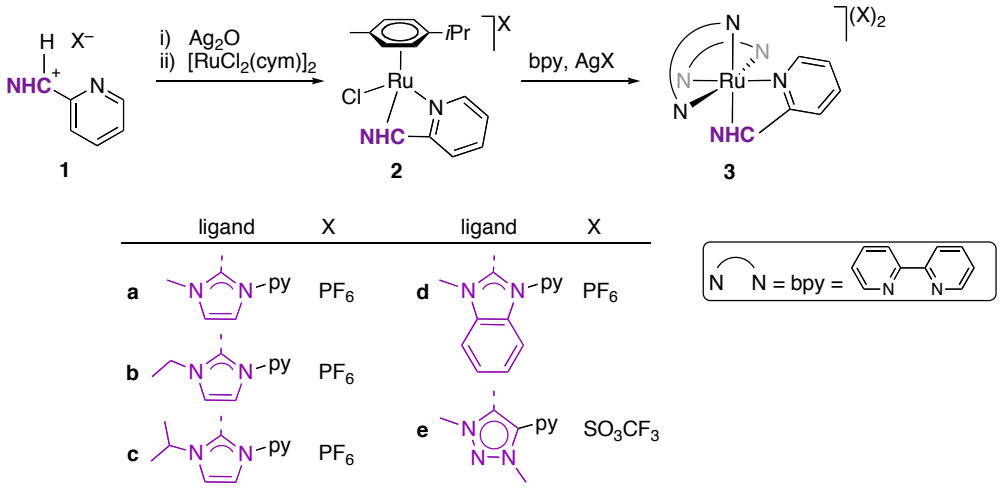

Complex **2a** was analysed by X-ray diffraction analysis. The molecular structure (Fig. 1) confirmed the expected ligand bonding and revealed the typical piano-stool geometry with a *N,C*-bidentate chelating pyridyl-carbene ligand. The ligand bite angle is 76.42(7)°, similar to the corresponding angle in related complexes, and essentially identical to the bite angle in **2e** (76.53(4)°).[19c] The Ru–C and Ru–N bonds are 2.009(2) and 2.092(18) Å, respectively, and both about 0.03 Å shorter than in **2e**. The pyridyl and NHC heterocycles are essentially co-planar, with a torsion angle of –1.6°.

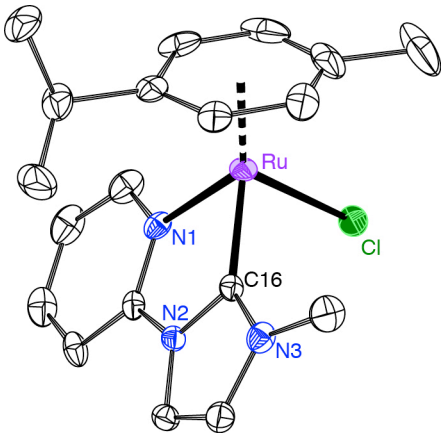

Figure 1 ORTEP representation of complex **2a** (50% probability level; hydrogen atoms and non-coordinated PF_6 anion omitted for clarity). Selected bond lengths and angles: Ru1–C16 2.009(2) Å, Ru1–N1 2.092(18) Å, Ru1–Cl 2.401(6) Å, Ru–$C_{centroid}$ 1.710(1) Å; C16–Ru1–N1 76.42(7)°.

Subsequent displacement of the *p*-cymene and chloride ligands in **2a–e** with 2,2'-bipyridine (bpy) was accomplished by heating a DMSO solution of the complexes in the presence of bpy and $AgPF_6$ (**2a–d**) or AgOTf (**2e**).[20] Under these conditions, the pyridyl-carbene ligand remained bound to the metal center.[17] Coordination of bpy induced a color change of the complexes from orange to a dark fluorescent red. Complexes **3a–e** are highly air and water stable for months, and neither the reaction nor the purifcation require anaerobic conditions. Generally, the complexes were purified by column chromatography using Al_2O_3 as stationary phase. While these complexes are chiral, no attempts were made to separate the *Δ* and *Λ* enantiomers.

Coordination of two bpy ligands was indicated in the ^{1}H NMR spectra by the loss of the *p*-cymene signals, and the emergence of 16 new proton signals in the aromatic region due to the non-equivalent pyridyl units. In the ^{13}C NMR spectra, the carbene carbons shift slightly downfield upon bpy coordination, a trend that was also observed when preparing the corresponding picolyl-carbene ruthenium complexes.[17] The carbene-linked pyridine moiety was assigned by nuclear Overhauser effects (NOEs) and by 2D NMR experiments. In all complexes **3a–e**, the four pyridyl protons of the carbene-bound pyridyl unit are shifted substantially upfield as compared with the corresponding protons of the bpy ligands. An enhanced shielding is presumably induced by the electron-rich properties of the *N*-heterocyclic carbene. For example in complex **3a**, the bpy protons bound to C3 appear as doublets in the 8.81–8.72 ppm range, whereas the analogous C3-bound proton of the NHC-substituted pyridyl resonates as low as 8.28 ppm. Such trends were consistently observed for all pyridyl protons in complexes **3a–e**.

A substantial upfield shift was also noted for the NHC wingtip groups of all five complexes upon bpy coordination. For example, the CH_3 group appeared at δ_H 4.11 ppm in the *p*-cymene complex **2a**, yet more than one ppm lower in **3a** (δ_H 3.03 ppm). Similarly, the CH_3 resonance of the ethyl substituent shifts from δ_H 1.48 ppm in **2b** to δ_H 0.72 ppm in the bpy complex **3b**. An almost identical difference was observed for one of the terminal CH_3 groups of the isopropyl wingtip substituent (δ_H 1.41 ppm in **2c** *vs* δ_H 0.68 ppm in **3c**, $\Delta\delta$ = 0.73 ppm). The other CH_3 unit experiences much less change ($\Delta\delta$ = 0.41 ppm), suggesting a bpy ligand is in closer vicinity to one methyl group than to the other.

Single crystals suitable for X-ray diffraction were obtained for **3a**. Despite the good quality of the crystals, refinement consistently converged to a $[Ru(bpy)_3]^{2+}$ complex. This composition was confidently excluded by NMR and MS analysis of the single crystals, which unambiguously revealed the presence of the pyridyl-carbene ligand. Hence, a complete disorder of the carbene ligand over all six coordination sites of ruthenium was concluded, which is in agreement with the relatively poor R values of the refined structure and the relatively unsharp intensity pattern. This conclusion suggests that the steric demand of the carbene-pyridyl ligand is highly similar to that of a bpy ligand (Fig. S3), rendering the carbene an excellent structural substitute, though obviously with different electronic implications.

Attempts to grow single crystals of complexes with sterically more demanding carbenes (*e.g.* **3c**, **3d**) for X-ray diffraction analysis have failed thus far.

Spectroscopic and electrochemical properties. The electronic impact of the pyridyl-carbene ligand was evaluated by comparing the spectroscopic and electrochemical properties of complexes **3a–e** to those of $[Ru(bpy)_3]^{2+}$.[21] All complexes **3a–e** showed absorption bands in the UV-vis spectrum that are reminiscent of those of $[Ru(bpy)_3]^{2+}$, comprising a strong absorption in the high UV range (< 300 nm) and a less strong band in the visible region with a λ_{max} in the 410–470 nm range (Table 1, Fig. S1). By comparison, these bands were attributed to ligand-centered π–π^* transitions and to metal-to-ligand charge transfer bands, respectively. The absorption in the visible range featured in all cases two maxima in close proximity (Fig. 2). The extinction coefficient of the visible band is largest for $[Ru(bpy)_3]^{2+}$ (ε = 10,300 and 11,500 $M^{-1}cm^{-1}$) and significantly smaller for the imidazolylidene-derived carbene complexes **3a–d** (ε = 1,800–5,000 $M^{-1}cm^{-1}$). The triazole complex **3e** displays the largest extinction coefficient of all the NHC complexes studied (ε = 8,160 and 7,900 $M^{-1}cm^{-1}$), only slightly smaller than that of $[Ru(bpy)_3]^{2+}$. In addition, the absorption band is broader and features a ca. 20 nm more bathochromic tail than $[Ru(bpy)_3]^{2+}$. This red shift is presumably induced by the stronger donation of the triazolylidene ligand,[22] which enhances the backbonding to the bpy ligands in agreement with the MLCT assignment of this band. This broader absorption band further suggests a potential for capturing also lower-energy sunlight with **3e** to access relevant excited states.

Table 1. Spectroscopic and Electrochemical Data for complexes **3a–e**

Complex	τ /ns [a]	λ_{max} /nm (ε / $M^{-1}cm^{-1}$) [b]	$E_{1/2}$ /V (ΔE_p / mV) [c]	
3a	187	414 (2,300), 445 (2,280)	+1.23 (69)	–1.36 (79)
3b	334	442 (4,580), 445 (4,980)	+1.01 [d]	–1.35 (30)
3c	333	404 (5,600), 430 (5,900)	+0.96 [d]	–1.34 (80)
3d	50	414 (4,350), 430 (4,190)	+1.32 (95)	–1.34 (96)
3e	188	430 (8,160), 464 (7,900)	+1.09 (63)	–1.32 (54)

$[Ru(bpy)_3]^{2+}$	530	424 (10,300), 450 (11,500)	+1.39 (55)	–1.27 (69)

[a] excitation at 355 (±3) nm in MeCN; [b] in MeCN; [c] in MeCN, sweep rate 100 mV s^{-1}, referenced to Fc^+/Fc, $E_{1/2}$ = 0.41 V (ΔE_p = 72 mV) with $\Delta E_p = E_{pa} - E_{pc}$), second reduction not always resolved; [d] anodic peak potential of irreversible oxidation.

Room temperature emission studies were carried out in CH_3CN using 355 nm excitation. All complexes are emissive at room temperature, with emission maxima in the range 610–620 nm. Complexes **3b** and **3c** with the most sterically demanding wingtip groups have the longest-lived lifetimes at 334 and 333 ns, respectively. Shorter excited state lifetimes were recorded for complex **3a** and **3e,** which have only a methyl substituent (187 and 188 ns, respectively). Complex **3d** comprised of a benzimidazole-derived carbene ligand revealed the shortest lifetime (50 ns).[23] Possibly, larger wingtip groups are important for extending the lifetime of these complexes. However, these bulky substituents were found to adversely affect red-ox properties and thus may not be beneficial (see below). Even though the excited state lifetimes of the carbene-modified complexes **3a–e** are all shorter than that of $[Ru(bpy)_3]^{2+}$, the values are within the same order of magnitude, perhaps with the exception of **3d** which displays a ten-fold shorter lifetime. In general, these lifetimes are thus long enough to allow for charge separation and electron injection into the conduction band of a semiconductor.[24]

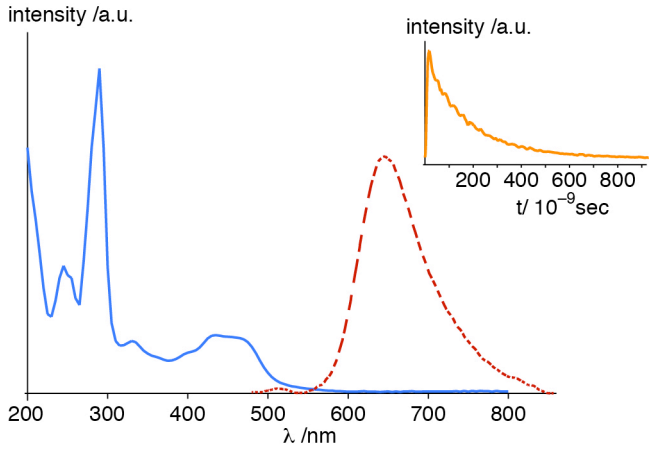

Figure 2 Absorption (blue solid line) and emission spectrum (red dashed line) upon excitation at 355 nm and intensity decay (inset) for **3e** in MeCN.

The impact of the carbene ligand was further investigated electrochemically by cyclic and differential pulse voltammetry. Complexes **3a**, **3d** and **3e** showed a reversible, presumably ruthenium-centered oxidation at $E_{1/2}$ = +1.23, +1.32 and +1.09V *vs*. SCE, respectively (Table 1, Fig. 3). All three potentials are lower than that of the parent $[Ru(bpy)_3]^{2+}$ complex, reflecting the stronger donor properties of a carbene as compared to a pyridine. Moreover, the donor properties of the different carbenes deduced by Tolman electronic parameters, pK_a analyses, and other techniques are clearly reflected in these oxidation potentials,[25] supporting the strongest donor properties for the triazolylidene and weakest for the benzimidazolylidene in this series.[22] In contrast to these complexes featuring methyl wingtip groups on the NHC ligand, complexes **3b** and **3c** with larger wingtip substituents display an irreversible oxidation with anodic peak potentials at E_{pa} = +1.01 V and +0.96 V, respectively (Table 1, Fig. S2). The trend in oxidation potentials correlates with the expected impact of the N-bound substituents. The irreversibility of the oxidation process is probably associated with the steric demand of the wingtip group and the ensuing congestion due to the proximity of one of the bpy heterocycles, which should induce a substantial distortion of the octahedral coordination geometry (*cf* NMR discussion). Complex **3d** does not show a significant improvement over $[Ru(bpy)_3]^{2+}$ in terms of redox properties. Considering the very short lifetime of its excited state and its poor absorption properties compared to the other carbene systems, the benzimidazolylidene motife appears to provide the least benefit for application in light to energy conversion devices.

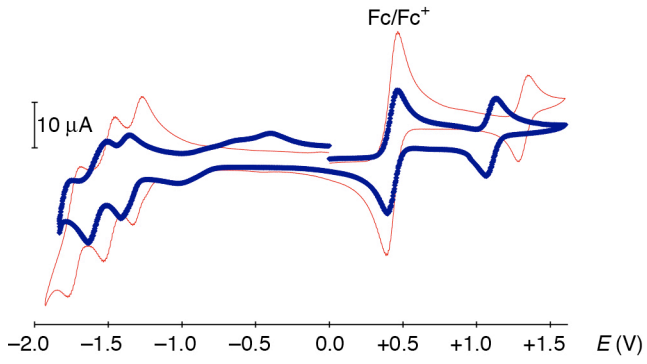

Figure 3 Cyclic voltammogram of $[Ru(bpy)_3](PF_6)_2$ (red thin line) and complex **3e** (blue bold line) in

MeCN with ferrocene as internal standard ($E_{1/2}$ (Fc/Fc^+) = 0.41 V vs. SCE).

All complexes also display a reversible reduction at around –1.3 V, and a second reduction around –1.5 V, albeit not always well-resolved. Similar values were observed with the tris(bipyridine) complex and have been ascribed to ligand-centered reductions.[9,21] Accordingly, the bpy ligand in complexes **3a–e** behaves as an electron acceptor ligand and is only marginally affected by the introduction of an NHC ligand, while the ruthenium(II) center as the electron donor site is modular and responds directly to the substitution of a pyridine by a carbene ligand. As a consequence, the HOMO–LUMO gap in the carbene complexes is substantially lowered upon introducing a carbene ligand. This effect is most pronounced in the triazolylidene ruthenium complex **3e** with a HOMO–LUMO gap of 2.41 eV, corresponding to a 10% reduction of the gap compared to $[Ru(bpy)_3]^{2+}$ (ΔE = 2.66 eV). This reduced energy gap is expected to be beneficial for photovoltaic applications, specifically in facilitating the charge separation process.[26]

Due to the favorable electrochemical and photophysical properties of complex **3e**, efforts have been directed towards the synthesis of a triazolylidine complex that would be suitable for immobilization on a photoanode as potential photosensitizer. Such immobilization has been achieved for example through the introduction of a carboxylate-functionalized bpy ligand, or by installing SCN^- ligands on the ruthenium center. Complex **5** features two solvento ligands and hence provides this flexibility to introduce an adsorption-active ligand at a late stage (Scheme 2). Complex **5** was prepared from complex **2e** in a stepwise protocol, involving first the displacement of the cymene and chloride ligands with MeCN according to established protocols, followed by the introduction of one bpy ligand to complex **4** in a hot DMSO solution. Complex **5** was fully characterized and featured less complex NMR spectra than complex **3e** due to the presence of only one bpy ligand. Most diagnostic for the introduction of only one bpy ligand is a strongly deshielded bpy proton (δ_H = 10.05 ppm) and a carbenic ^{13}C NMR resonance at rather high field (δ_C = 170.5 ppm). Unambiguous confirmation of the structure of complex

5 was obtained from a single crystal X-ray diffraction analysis. The molecular structure features a distorted octahedral geometry around the ruthenium center (Fig. 4). Both sulfur atoms are *S*-bound and are coordinated *trans* to pyridine units. The Ru–$C_{carbene}$ bond is 2.064(4) Å, slightly longer than in complex **2a** (2.009(2) Å). Only slight differences in the Ru–Nbpy bonds are observed (Ru-N1 2.137(3) Å, Ru-N2 2.111(3) Å), despite the two distinctly different *trans* influencing ligands.

Scheme 2

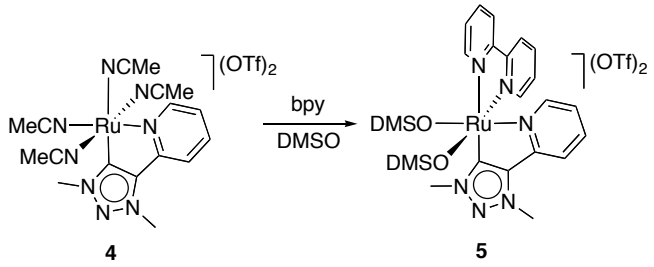

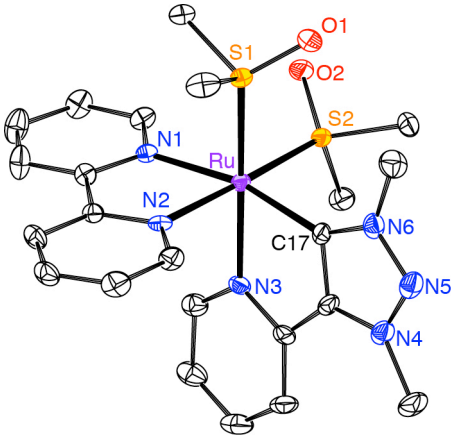

Figure 4 ORTEP representation of complex **5** (50% probability level, hydrogen atoms and the two non-coordinated PF_6^- anions omitted for clarity). Selected bond lengths and angles: Ru1-C17 2.064(4) Å, Ru1-N3 2.149(2) Å, Ru1-N2 2.111(3) Å, Ru1-N1 2.137(3) Å, Ru1-S1 2.262(6) Å, Ru1-S2 2.2684(9) Å, C17-Ru1-N3 77.99(13)°, N1-Ru1-N2 77.50(12)°, S1-Ru1-S2 89.14(3)°.

Conclusions

Five novel ruthenium (II) polypyridine complexes have been prepared. Electrochemical

measurements show that the presence of an NHC strongly assists oxidation processes. This may be beneficial over tris(bipyridine) ruthenium and its analogues in charge separation for use in DSSCs.[12] UV vis measurements show that these altered complexes absorb less strongly than the parent compound $Ru(bpy)_3^{2+}$, but within the same region. All of the complexes emit at room temperature with slightly shorter lifetimes compared to the parent compound, but promisingly were in the same range. The triazolylidene ruthenium system features the smallest HOMO-LUMO gap, with reasonable extinction coefficients and excited-state lifetimes that are attractive for photosensitization, thus warranting testing of these complexes for use as dyes in solar cells. This work may therefore provide guidelines for the fabrication of optimized DSSCs with higher efficacy.

Experimental Section

General comments. The synthesis of 1-ethylimidazole, the azolium salts **1a**, **1c–e**, and complexes **2e** and **4** are reported elsewhere.[19c,27] All other starting materials and reagents were obtained from commercial sources and used as received unless otherwise stated. NMR spectra were recorded on Varian spectrometers operating at 300–600 MHz. Chemical shifts δ are reported in ppm (*J* in Hz) relative to Me_4Si or residual protio solvents. Signals were assigned with the aid of two-dimensional cross-coupling experiments. UV-vis spectra were recorded on a Varian 50 Spectrophotometer. Elemental analysis was performed on an Exeter Analytical CE440 elemental analyser. High-resolution mass spectrometry was carried out with a Micromass/Waters Corp. USA liquid chromatography time-of-flight spectrometer equipped with an electrospray source.

Electrochemical studies were carried out using a Metrohm Autolab Potentiostat Model PGSTAT101 employing a gas-tight three electrode cell under an argon atmosphere. A platinum disk with 7.0 mm^2 surface area was used as the working electrode and polished before each measurement. The reference electrode was Ag/AgCl, the counter electrode was a Pt foil. In all experiments Bu_4NPF_6 (0.1 M in dry CH_3CN) was used as supporting electrolyte with analyte concentrations of approximately 1 mM. The

ferrocenium/ferrocene redox couple was used as an internal reference ($E_{1/2}$ = 0.46 V vs. SCE).[28]

Emission spectra (accuracy ±3 nm) were recorded at 298 K using a LS50B luminescence spectrophotometer, equipped with a red sensitive Hamamatsu R928 PMT detector, interfaced with an Elonex PC466 employing Perkin-Elmer FL WinLab custom built software. The laser flash photolysis apparatus has been described previously.[29] For this work, the 355 nm line of a pulsed Nd:YAG laser was used (energy approximately 35 mJ per pulse; system response 10 ns). Solutions for analysis were placed in a fluorescence cuvette (d = 1 cm) and were degassed by purging with argon for 20 mins. The absorbance of the solution at the excitation wavelength was adjusted to lie in the range 0.18–0.2. The UV/Vis. spectrum of the sample solution was monitored throughout the experiments to monitor changes in absorbance.

***N*-ethyl-*N'*-(2-pyridyl)-imidazolium hexafluoro phosphate (1b).** 1-ethyl imidazole (0.98 g, 10 mmol) and 2-bromopyridine (1.60 g, 10 mmol) were stirred at 160 °C for 24 h. MeOH was added and the salt was precipitated from Et_2O. The salt was dissolved in a saturated solution of NH_4PF_6, and the product was extracted with CH_2Cl_2. The organics were dried over $MgSO_4$, filtered and volatiles removed under vacuo. Repeated precipitation from CH_3CN/Et_2O gave the desired product as an off- white powder in 0.76g, 30% yield. ^{1}H NMR (DMSO-D_6, 500 MHz): δ = 10.09 (s, 1H, NC*H*N), 8.64 (d, 1H, $^3J_{HH}$ = 4.8 Hz, H_{pyr}), 8.51 (d, 1H, $^3J_{HH}$ = 1.8 Hz, H_{im}), 8.21 (t, 1H, $^3J_{HH}$ = 7.6 Hz, H_{pyr}), 8.07 (d, 1H, $^3J_{HH}$ = 1.8 Hz, H_{im}), 8.03 (d, 1H, $^3J_{HH}$ = 7.6 Hz, H_{pyr}), 7.63 (dd, 1H, $^3J_{HH}$ = 4.8 Hz, $^3J_{HH}$ = 7.6 Hz, H_{pyr}), 4.32 (q, 2H, $^3J_{HH}$ = 7.3 Hz, CH_2), 1.50 (t, 1H, $^3J_{HH}$ = 7.3 Hz, CH_3). ^{13}C{^{1}H} NMR (DMSO-D_6, 125 MHz): δ = 149.2 (C_{pyr}H), 146.1 (C_{pyr}), 140.6 (C_{pyr}H), 133.8 (NCN), 125.65 (C_{pyr}H), 123.21 (C_{im}H), 120.15 (C_{im}H), 114.97 (C_{pyr}H), 44.89 (NCH_2), 14.82 (CH_3). Elemental analysis calcd for $C_{10}H_{12}F_6N_3$ (319.06) × H_2O: C 39.22, H 4.61, N 13.72; found: C 39.70, H 4.54, N 13.66.

***κ*^{2}-*C,N*-(*N*-methyl-*N'*-(2-pyridyl)-imidazol-2-ylidene)ruthenium(p-cymene)chloride**

hexafluorophosphate (2a). To a solution of **1a** (152 mg, 0.50 mmol) in CH_3CN (30 mL) was added Ag_2O (60 mg, 0.26 mmol), and the mixture stirred under exclusion of light and for 72 h at 45 °C. The suspension was filtered through a pad of Celite and concentrated to 5 mL. A solution of $[RuCl_2(p\text{-cymene})]_2$ (153 mg, 0.25 mmol) in CH_2Cl_2 (20 mL) was added and the mixture was stirred for 4 h at room temperature. The formed white precipitate was removed by filtration over Celite. Addition of Et_2O (200 mL) to the filtrate induced precipitation of the product, which was collected by centrifugation and purified by column chromatography (SiO_2, CH_3CN/H_2O 9:1) to yield **2a** as a yellow powder (241 mg, 82%). Single crystals were grown from slow diffusion of pentane into a CH_2Cl_2 solution of **2a**. ^{1}HNMR (DMSO-D_6, 600 MHz): δ = 9.33 (dd, 1H, $^3J_{HH}$ = 5.7 Hz, $^4J_{HH}$ = 1.0 Hz, H_{pyr}), 8.39 (d, 1H, $^3J_{HH}$ = 1.8 Hz, H_{im}), 8.24 (td, 1H, $^3J_{HH}$ = 8.4 Hz, $^4J_{HH}$ = 1.0 Hz, H_{pyr}), 8.15 (d, 1H, $^3J_{HH}$ = 8.4 Hz, H_{pyr}), 7.79 (d, 1H, $^3J_{HH}$ = 1.8 Hz, H_{im}), 7.51 (dd, 1H, $^3J_{HH}$ = 8.4 Hz, $^3J_{HH}$ = 5.7 Hz, H_{pyr}), 6.39, 6.35, 6.16, 5.74 (4 × d, 1H, $^3J_{HH}$ = 6.3 Hz, H_{cym}), 4.11 (s, 3H, NCH_3), 2.36 (septet, 1H, $^3J_{HH}$ = 6.9 Hz, $CHMe_2$), 2.11 (s, 3H, cym-CH_3), 0.85, 0.83 (2 × d, 6H, $^3J_{HH}$ = 6.9 Hz, CHCH_3). ^{13}C{^{1}H} NMR (DMSO-D_6, 150 MHz): δ = 181.0 (C–Ru), 155.7 (C_{pyr}H), 151.3 (C_{pyr}), 141.5 (C_{pyr}H), 126.3 (C_{im}H), 122.8 (C_{pyr}H), 116.5 (C_{im}H), 112.1 (C_{pyr}H), 103.3, 98.1 (2 × C_{cym}), 90.8, 90.6, 86.4, 81.3 (4 × C_{cym}H), 37.8 (NCH_3), 30.35 (cym–$CHMe_2$), 22.1, 21.7 (2 × CHCH_3), 18.5 (cym–CH_3). Elemental analysis calcd for $C_{19}H_{23}ClF_6N_3PRu$ (574.89): C 39.69, H 4.02, N 7.30; found: C 39.68, H 4.04, N 7.33. HR-MS (m/z): 430.0613, calcd for $[M–PF_6]^+$ 430.0623.

***κ*^{2}-*C*,*N*-(*N*-ethyl-*N'*-(2-pyridyl)-imidazol-2-ylidene)ruthenium(p-cymene)chloride hexafluorophosphate of (2b).** Complex **2b** was prepared according to the method described for **2a**, starting from compound **1b** (100 mg, 0.39 mmol), Ag_2O (90 mg, 0.39 mmol), $[RuCl_2(p\text{-cymene})]_2$ (119 mg, 0.19 mmol) in CH_2Cl_2 (20 mL) and was obtained as a red powder (100 mg, 60%). Analytically pure material was obtained by recrystallization from MeCN and Et_2O. ^{1}H NMR (DMSO-D_6, 400 MHz): δ = 9.31 (d, 1H, $^3J_{HH}$ = 6.2 Hz, H_{pyr}), 8.43 (d, 1H, $^3J_{HH}$ = 1.9 Hz, H_{im}), 8.23 (dd, 1H, $^3J_{HH}$ = 8.7 Hz, $^3J_{HH}$ = 7.0 Hz, H_{pyr}), 8.14 (d, 1H, $^3J_{HH}$ = 8.7 Hz, H_{pyr}), 7.87 (d, 1H, $^3J_{HH}$ = 1.9 Hz, H_{im}), 7.49 (dd, 1H, $^3J_{HH}$ = 6.2 Hz,

$^3J_{HH}$ = 8.7 Hz, H_{pyr}), 6.31 (2 × d, 2H, $^3J_{HH}$ = 6.0 Hz, H_{cym}), 6.17 (d, 1H, $^3J_{HH}$ = 6.0 Hz, H_{cym}), 5.70 (d, 1H, $^3J_{HH}$ = 5.1 Hz, H_{cym}), 4.44 (q, 2H, $^3J_{HH}$ = 6.8 Hz, NCH_2), 2.30 (septet, 1H, $^3J_{HH}$ = 6.8 Hz, cym-$CHMe_2$), 2.09 (s, 3H, cym-CH_3), 1.48 (t, 3H, $^3J_{HH}$ = 6.8 Hz, NCH_2CH_3), 0.83, 0.80 (2 × d, 6H, $^3J_{HH}$ = 6.8 Hz, cym-$CHCH_3$). $^{13}C\{^1H\}$ NMR (DMSO-D_6, 125MHz): δ = 195.2 (C-Ru), 156.1 ($C_{pyr}H$), 151.7 (C_{pyr}), 142.0 ($C_{pyr}H$), 125.0 ($C_{im}H$), 123.4 ($C_{pyr}H$), 117.4 ($C_{im}H$), 112.7 ($C_{pyr}H$), 109.3, 101.1 (2 × C_{cym}), 91.4, 86.5, 82.3 (4 × $C_{cym}H$), 46.4 (NCH_2), 30.8 (cym–$CHMe_2$), 22.7, 22.1 (2 × cym–$CHCH_3$), 19.0 (cym–CH_3), 16.3 (NCH_2CH_3). Elemental analysis calcd for $C_{20}H_{25}ClF_6N_3PRu$ (589.04) × 2 CH_3CN: C 42.89, H 4.80, N 10.42; found: C 43.10, H 5.29, N 10.38. HR-MS (m/z): 444.0762, calculated for $[M–PF_6]^+$ 444.0781.

***κ*²-*C*,*N*-(*N*-isopropyl-*N'*-(2-pyridyl)-imidazol-2-ylidene)ruthenium(p-cymene)chloride hexafluorophosphate (2c).** Complex **2c** was prepared by the method described for **2a** starting from **1c** (78 mg, 0.29 mmol) and Ag_2O (67 mg, 0.29 mmol) in CH_2Cl_2 (10 mL) and using $[RuCl_2(p\text{-cymene})]_2$ (89 mg, 0.14 mmol), affording the title product as a red powder (0.13 g, 46%). An analytically pure sample was obtained by slow diffusion of Et_2O into a solution of **2a** in CH_2Cl_2. ^1H NMR (DMSO-D_6, 500 MHz): δ = 9.32 (d, 1H, $^3J_{HH}$ = 5.8 Hz, H_{pyr}), 8.49 (d, 1H, $^3J_{HH}$ = 2.2 Hz, H_{im}), 8.24 (t, 1H, $^3J_{HH}$ = 8.2 Hz, H_{pyr}), 8.15 (d, 1H, $^3J_{HH}$ = 8.2 Hz, H_{pyr}), 8.03 (d, 1H, $^3J_{HH}$ = 2.2 Hz, H_{im}), 7.50 (dd, 1H, $^3J_{HH}$ = 5.8 Hz, $^3J_{HH}$ = 8.2 Hz, H_{pyr}), 6.32, 6.23, 6.13, 5.71 (4 × d, 1H, J_{HH} = 5.0 Hz, H_{cym}), 4.96 (septet, 1H, $^3J_{HH}$ = 6.6 Hz, $NCHMe_2$), 2.33 (septet, 1H, $^3J_{HH}$ = 6.9 Hz, cym-$CHMe_2$), 2.12 (s, cym-CH_3), 1.72, 1.40 (2 × d, 3H, $^3J_{HH}$ = 6.6 Hz, $NCHCH_3$), 0.86, 0.84 (2 × d, 6H, $^3J_{HH}$ = 6.9 Hz, cym-$CHCH_3$). $^{13}C\{^1H\}$ NMR (DMSO-D_6, 125MHz): δ = 182.3 (C-Ru), 155.7 ($C_{pyr}H$), 151.2 (C_{pyr}), 141.5, 122.8 (2 × $C_{pyr}H$), 121.4, 117.6 (2 × $C_{im}H$), 112.1 ($C_{pyr}H$), 108.5, 104.1 (2 × C_{cym}), 91.0, 86.5, 85.2 (4 × $C_{cym}H$), 53.8 ($NCHMe_2$), 30.8 (cym–$CHMe_2$), 23.8, 22.8 (2 × $NCHCH_3$), 21.3 (cym-$CHMe_2$), 18.3 (cym-CH_3). Elemental analysis calcd for $C_{21}H_{27}ClF_6N_3PRu$ (603.06) × Et_2O: C 43.54, H 5.18, N 6.35; found: C 43.69, H 4.74, N 6.63. HR-MS (m/z): 458.0923, calculated for $M–PF_6]^+$ 458.0937.

***κ*²-*C*,*N*-(*N*-methyl-*N'*-(2-pyridyl)-benzimidazol-2-ylidene)ruthenium(p-cymene)chloride hexafluorophosphate (2d).** Compound **1d** (250 mg, 0.70 mmol) and Ag_2O (81.6 mg, 0.35 mmol) were dissolved in CH_3CN (20 mL) and stirred at 60 °C for 48 h in the absence of light. This solution was filtered through a pad of Celite. Solid $[RuCl_2(p\text{-cymene})]_2$ (214 mg, 0.35 mmol) was added to the filtrate and the mixture was stirred at 60 °C for a further 24 h in the absence of light. The resulting suspension was filtered through a pad of Celite and the filtrate evaporated to dryness. The residue was purified by precipitation from CH_2Cl_2/Et_2O (30 mL/200 mL) and subsequently by column chromatography (SiO_2, CH_3CN/H_2O 9:1) to give **2d** as a red powder (0.20 g, 60%). Analytical pure **2d** was obtained by recrystallization from MeOH and Et_2O. ^1H NMR (DMSO-D_6, 500 MHz): δ = 9.44 (d, 1H, $^3J_{HH}$ = 6.5 Hz, H_{pyr}), 8.53 (d, 1H, $^3J_{HH}$ = 9.0 Hz, H_{benz}), 8.43 (m, 2H, H_{pyr}), 8.29 (d, 1H, $^3J_{HH}$ = 8.5 Hz, H_{benz}), 8.01 (m, 2H, H_{benz}), 7.64 (t, 1H, $^3J_{HH}$ = 6.5 Hz, H_{pyr}), 6.50 (2 x d, 2H, $^3J_{HH}$ 5.0 Hz H_{cym}), 6.29 , 5.91 (2 × d, 1H, $^3J_{HH}$ = 5.0 Hz, H_{cym}), 4.35 (s, 3H, NCH_3), 2.40 (septet, 1H, $^3J_{HH}$ =4.5 Hz, cym–$CHMe_2$), 2.16 (s, 3H, cym–CH_3), 0.97, 0.95 (2 × d, 6H, $^3J_{HH}$ = 4.5 Hz, CHC*H*$_3$). $^{13}C\{^1H\}$ NMR (DMSO-D_6, 125 MHz): δ = 197.5 (C–Ru), 156.1 ($C_{pyr}H$), 151.1 (C_{pyr}), 141.6 ($C_{pyr}H$), 135.7 (C_{benz}), 129.2, (C_{benz}), 125.8, 125.2, 125.0 (3 × $C_{benz}H$), 122.4 (C_{benz}), 112.8 ($C_{pyr}H$), 112.4 ($C_{benz}H$), 112.0 ($C_{pyr}H$), 92.6, 92.0, 88.4, 82.9 (4 × $C_{cym}H$), 35.4 (NCH_3), 30.3 (cym–$CHMe_2$), 21.8, 21.7 (2 × CH*C*H_3), 18.1 (cym–CH_3). Elemental analysis calcd for $C_{23}H_{25}ClF_6N_3PRu$ (624.95) × 0.5 H_2O: C 43.57, H 4.13, N 6.63; found: C 43.57, H 4.77, N 6.92. HR-MS (m/z): 480.0797, calculated for $[M–PF_6]^+$ 480.0781.

General procedure for the synthesis of complexes 3a–e. Ruthenium complex **2**, 2,2'-bipyridine (2 equiv), and $AgPF_6$ (2 equiv) were stirred in DMSO (6 mL) at 120 °C for 15 h in the absence of light. After cooling to room temperature, the solution was filtered through a pad of Celite. A red precipitate formed upon addition of CH_2Cl_2 (30 mL) and Et_2O (200 mL), which was collected and purified by column chromatography (neutral Al_2O_3, CH_3CN/H_2O 9:1). Analytically pure samples were obtained by

recrystallization from CH_2Cl_2 or MeCN and Et_2O.

***κ*²-*C*,*N*-(*N*-methyl-*N'*-(2-pyridyl)-imidazol-2-ylidene)bis(2,2'-bipyridine)ruthenium bis(hexafluorophosphate) (3a).** The general procedure starting from complex **2a** (100 mg, 0.17 mmol), 2,2'-bipyridine (54.2 mg, 0.34 mmol) and $AgPF_6$ (85.6 mg, 0.34 mmol) afforded **3a** as a red powder (129 mg, 88%). ^{1}H NMR (DMSO-D_6, 600 MHz): δ = 8.81, 8.76, 8.72 (4 x d, 4H, $^3J_{HH}$ 8.2 Hz, H^3_{bpy}), 8.56 (d, 1H, $^3J_{HH}$ 2.3 Hz, H_{im}), 8.28 (d, 1H, $^3J_{HH}$ 8.3 Hz, H^3_{pyr}), 8.22, 8.17, 8.12 (4 x td, 4H, $^3J_{HH}$ 8.2 Hz, $^4J_{HH}$ 1.3 Hz, H^4_{bpy}), 8.08 (td, 1H, $^3J_{HH}$ 8.2 Hz, $^4J_{HH}$ 1.3 Hz, H^4_{pyr}),7.97, 7.78, 7.65 (3 x d, 3H, $^3J_{HH}$ 5.6 Hz, H^6_{bpy}), 7.62 (ddd, 1H, $^3J_{HH}$ 8.2 Hz, $^3J_{HH}$ 5.6 Hz, $^4J_{HH}$ 1.3 Hz H^5_{bpy}), 7.58 (d, 1H, $^3J_{HH}$ 5.6 Hz, H^6_{pyr}), 7.52, 7.49, 7.44 (3 x ddd, 3H, $^3J_{HH}$ 8.2 Hz, $^3J_{HH}$ 5.6 Hz, $^4J_{HH}$ 1.3 Hz, H^5_{bpy}), 7.28 (ddd, 1H, $^3J_{HH}$ 8.2 Hz, $^3J_{HH}$ 5.6 Hz, $^4J_{HH}$ 1.3 Hz, H^5_{pyr}), 3.03 (s, 3H, CH_3). $^{13}C\{^1H\}$ NMR (DMSO-D_6, 150 MHz): δ = 192.3 (C-Ru), 156.4, 156.3, 156.1 (3 × C^2_{bpy}), 155.5 (C^6_{pyr}), 155.3 (C^2_{bpy}), 153.7 (C^2_{pyr}), 151.7 (C^6_{bpy}), 151.4 (C^6_{bpy}), 151.4 (C^6_{bpy}), 149.2 (C^6_{bpy}), 140.1 (C^4_{bpy}), 139.1 (C^4_{bpy}), 138.0 (C^4_{pyr}), 137.8 (C^4_{bpy}), 137.7 (C^4_{bpy}), 128.5 (C^5_{bpy}), 128.6 (C^5_{bpy}), 128.3 (C^5_{bpy}), 128.1 (C^5_{bpy}), 127.8 (C^5_{bpy}), 126.7 ($C_{im}H$), 124.8 (C^3_{bpy}), 124.7 (C^3_{bpy}), 124.6 (C^3_{bpy}), 123.6 (C^3_{bpy}), 117.8 ($C_{im}H$), 112.7 (C^3_{pyr}), 35.1 (CH_3). Elemental analysis calcd for $C_{29}H_{25}F_{12}N_7P_2Ru$ (863.05): C 40.38, H 2.92, N 11.37; found: C 40.41, H 2.95, N 11.23. HR-MS (m/z): 286.5610, calculated for $[M–2PF_6]^{2+}$ 286.5607.

***κ*²-*C*,*N*-(*N*-ethyl-*N'*-(2-pyridyl)-imidazol-2-ylidene)bis(2,2'-bipyridine)ruthenium bis(hexafluorophosphate) (3b).** The product was obtained from **2b** (100 mg, 0.16 mmol), 2,2'-bipyridine (50 mg, 0.32 mmol) and $AgPF_6$ (80 mg, 0.32 mmol) as a red powder (79 mg, 56%). ^{1}H NMR (DMSO-D_6, 500 MHz): δ = 8.81- 8.84 (m, 2H, H^3_{bpy}), 8.78, 8.75 (2 x d, 2H, $^3J_{HH}$ 8.2 Hz, H^3_{bpy}), 8.65 (d, 1H, $^3J_{HH}$ = 2.3 Hz, H_{im}), 8.33 (d, 1H, $^3J_{HH}$ = 8.3 Hz, H^3_{pyr}), 8.22 (td, 1H, $^3J_{HH}$ = 8.2Hz, $^4J_{HH}$ = 1.5 Hz, H^4_{bpy}), 8.16 (2 x td, 2H, $^3J_{HH}$ 8.2 Hz, $^4J_{HH}$ unresolved, H^4_{bpy}), 8.12 (2 x td, 2H, $^3J_{HH}$ 8.2 Hz, $^4J_{HH}$ 1.5 Hz, $H^4_{bpy,}$ H^4_{pyr}), 7.94, 7.78, 7.72 (3 x d, 3H, $^3J_{HH}$ = 5.8 Hz, H^6_{bpy}), 7.68 (d, 1H, $^3J_{HH}$ = 2.3 Hz, H_{im}), 7.67 (d,

1H, $^{3}J_{HH}$ = 5.8 Hz, H^{6}_{bpy}), 7.61- 7.58 (m, 1H, H^{6}_{pyr}), 7.53- 7.48 (m, 4H, H^{5}_{bpy}), 7.44 (ddd, 1H, $^{3}J_{HH}$ = 8.2 Hz, $^{3}J_{HH}$ = 5.8 Hz, $^{3}J_{HH}$ = 1.5 Hz, H^{5}_{pyr}), 3.3 (q, 2H, $^{3}J_{HH}$ = 7.3 Hz, NCH_2), 0.75 (t, 3H, $^{3}J_{HH}$ = 7.3 Hz, $NCH_2C\mathit{H}_3$). $^{13}C\{^{1}H\}$ NMR (DMSO-D_6, 125MHz): δ = 205.7 (C-Ru), 156.6, 156.3, 156.1 (3 x C^{2}_{bpy}), 156.0 (C^{6}_{pyr}), 154.8 (C^{2}_{bpy}), 152.8 (C^{2}_{pyr}), 152.4 (C^{6}_{bpy}), 150.9 (C^{6}_{bpy}), 150.2 (C^{6}_{bpy}), 148.2 (C^{6}_{boy}), 139.8 (C^{4}_{bpy}), 137.7 (C^{4}_{bpy}), 136.5 ($C_{bpy}H$), 128.6 ($C_{bpy}H$), 128.3 ($C_{bpy}H$), 128.1 ($C_{pyr}H$), 128.0 ($C_{bpy}H$), 127.6 ($C_{bpy}H$), 125.2 ($C_{pyr}H$), 125.0 ($C_{bpy}H$), 124.9 ($C_{bpy}H$), 124.3 ($C_{bpy}H$), 124.0 ($C_{bpy}H$), 123.0 ($C_{bpy}H$), 120.6 ($C_{im}H$), 117.9 ($C_{im}H$), 109.4 (C^{3}_{pyr}), 41.1 (NCH_2), 23.0 ($NCH_2\mathit{C}H_3$). HR-MS (m/z): 293.5680, calculated for $[M–2PF_6]^{2+}$ 293.5685.

***κ*²-*C*,*N*-(*N*-isopropyl-*N'*-(2-pyridyl)-imidazol-2-ylidene)bis(2,2'-bipyridine)ruthenium bis(hexafluorophosphate) (3c).** The product was obtained from **2c** (100 mg, 0.16 mmol), 2,2'-bipyridine (50 mg, 0.32 mmol) and $AgPF_6$ (80 mg, 0.32 mmol) as a red powder (93 mg, 65%). ^{1}H NMR (DMSO-D_6, 600 MHz): δ = 8.86, 8.83, 8.82, 8.79 (4 x d, 4H, $^{3}J_{HH}$ 8.1 Hz, H^{3}_{bpy}), 8.75 (d, 1H, $^{3}J_{HH}$ 2.4 Hz, H_{im}), 8.36 (d, 1H, $^{3}J_{HH}$ 8.1 Hz, H^{3}_{pyr}), 8.23, 8.19 (2 x td, 2H, $^{3}J_{HH}$ 8.1 Hz, $^{4}J_{HH}$ 1.4 Hz, H^{4}_{bpy}), 8.14, 8.13 (2 x td, 2H, not resolved, H^{4}_{bpy}), 8.12 (td, 1H, $^{3}J_{HH}$ 8.1 Hz, $^{4}J_{HH}$ 1.4 Hz, H^{4}_{pyr}), 7.96 (d, 1H, $^{3}J_{HH}$ 6.4 Hz, H^{6}_{pyr}), 7.77, 7.67 (2 x d, 2H, $^{3}J_{HH}$ 6.4 Hz, H^{6}_{bpy}), 7.63, 7.62 (2 x d ddd, 2H, $^{3}J_{HH}$ 8.1 Hz, $^{3}J_{HH}$ 6.4 Hz, $^{4}J_{HH}$ 1.4 Hz H^{5}_{bpy}), 7.56- 7.53 (m, 2H, $H^{5}_{bpy,}$ H^{6}_{bpy}), 7.51 (d, 1H, $^{3}J_{HH}$ 6.4 Hz, H^{6}_{bpy}), 7.46 (ddd, 1H, $^{3}J_{HH}$ 8.1 Hz, $^{3}J_{HH}$ 6.4 Hz, $^{4}J_{HH}$ 1.4 Hz H^{5}_{bpy}), 7.28 (ddd, 1H, $^{3}J_{HH}$ 8.1 Hz, $^{3}J_{HH}$ 6.4 Hz, $^{4}J_{HH}$ 1.4 Hz H^{5}_{pyr}), 3.28 (septet, 1H, $^{3}J_{HH}$ = 6.7 Hz, $NCHMe_2$), 1.31, 0.68 (2 × d, 3H, $^{3}J_{HH}$ = 6.7 Hz). $^{13}C\{^{1}H\}$ NMR (DMSO-D_6, 150MHz): δ = 190.9 (C-Ru), 157.3, 157.2, 157.1 (3 × C^{2}_{bpy}), 156.7 (C^{6}_{pyr}), 155.6 (C^{2}_{bpy}), 155.4 (C^{2}_{pyr}), 154.4 (C^{6}_{bpy}), 151.5 (C^{6}_{bpy}), 150.9 (C^{6}_{bpy}), 149.5 (C^{6}_{bpy}), 140.5 (C^{4}_{bpy}), 139.4 (C^{4}_{bpy}), 138.5 (C^{4}_{pyr}), 138.4 (C^{4}_{bpy}), 138.2 (C^{4}_{bpy}), 128.8 (C^{5}_{bpy}), 128.7 (C^{5}_{bpy}), 128.5 (C^{5}_{bpy}), 128.4 (C^{5}_{bpy}), 128.2 (C^{5}_{bpy}), 125.3 (C^{3}_{bpy}), 124.9 (C^{3}_{bpy}), 124.8 (C^{3}_{bpy}), 123.68 (C^{3}_{bpy}), 121.9 (C_{im}), 119.4 (C_{im}), 113.1 (C^{3}_{pyr}), 51.1 ($NCHMe_2$), 23.5, 22.3 (2 × $NCH\mathit{C}H_3$). HR-MS (m/z): 300.5938, calculated for $[M–2PF_6]^{2+}$ 300.5764.No satisfactory elemental analysis was obtained for this complex; the best analyses were determined for an analogue of

3c containing BF_4^- counterions: calcd for $C_{31}H_{29}B_2F_8N_7Ru$ (589.04): C 48.09, H 3.78, N 12.66; found: C 47.95, H 4.63, N 12.94.

***κ*²-*C*,*N*-(*N*-methyl-*N'*-(2-pyridyl)-benzimidazol-2-ylidene)bis(2,2'-bipyridine)ruthenium bis(hexafluorophosphate) (3d).** The product was obtained from **2d** (100 mg, 0.16 mmol), 2,2'-bipyridine (50 mg, 0.32 mmol) and $AgPF_6$ (80 mg, 0.32 mmol) as a red powder (100 mg, 35%). ^{1}H NMR (DMSO-D_6, 500 MHz): δ = 8.86 (d, 1H, $^3J_{HH}$ 8.4 Hz, H^3_{bpy}), 8.78 (3 x d, 3H, unresolved, H^3_{bpy}), 8.68 (d, 1H, $^3J_{HH}$ 8.4 Hz, H^3_{pyr}), 8.48 (m, 1H, H_{benz}), 8.26 (td, 1H, $^3J_{HH}$ 8.4 Hz, $^4J_{HH}$ unresolved, H^4_{bpy}), 8.19-8.16 (m, 3H, 2 x H^4_{bpy} + H_{benz}), 8.13 (td, 1H, $^3J_{HH}$ 8.4 Hz, $^4J_{HH}$ unresolved, H^4_{pyr}), 7.81 (d, 1H, $^3J_{HH}$ = 5.5 Hz, H^6_{bpy}), 7.71- 7.69 (m, 1H, H_{benz}), 7.64 (2 x d, 2H, $^3J_{HH}$ = 5.5 Hz, H^6_{bpy}), 7.61 (d, 1H, $^3J_{HH}$ = 5.5 Hz, H^6_{bpy}), 7.55 (d, 1H, $^3J_{HH}$ = 5.5 Hz, H^6_{pyr}), 7.52-7.50 (m, 2H, H^5_{bpy} + H_{benz}), 7.49 (2 x d, ddd, 2H, $^3J_{HH}$ 6.5Hz, unresolved, H^5_{bpy}), 7.41 (ddd, $^3J_{HH}$ 6.5Hz, unresolved, H^5_{bpy}), 7.31 (ddd, $^3J_{HH}$ 6.5Hz, unresolved, H^5_{pyr}), 3.24 (s, 3H). ^{13}C {^{1}H} NMR (DMSO-D_6, 125MHz): δ = 206.1 (C-Ru), 156.6 (C^4_{pyr}), 155.9 (C^2_{bpy}), 154.9 (C^2_{bpy}), 154.7, 151.9 (C^6_{bpy}), 151.8 (C^6_{bpy}), 151.4 (C^6_{pyr}), 150.9 (C_{benz}), 148.8 (C^2_{bpy}), 140.4, 139.5 (C^4_{bpy}), 138.4 , 138.3 (C^4_{bpy}, CH_{benz}), 138.2 (C^4_{pyr}),131.4 (C_{benz}),, 128.6 (C^6_{bpy}), 128.4 (C^5_{bpy}), 128.1 (C^6_{bpy}), 128.0 (C^5_{bpy}),, 125.1 (C^5_{bpy}), 125.0 (C^3_{bpy}), 124.9 (C^3_{bpy}), 124.8 (C^3_{bpy}), 124.8 (C^5_{bpy}), 124.6 (C^3_{bpy}), 124.5 (C^5_{bpy}) (CH_{benz}), 123.2 (C^3_{pyr}), 113.6 (C^3_{pyr}), 112.4 (CH_{benz}), 112.1 (CH_{benz}), 32.39 (CH_3). Elemental analysis calcd for $C_{33}H_{27}F_{12}N_7P_2Ru$ (913.07) × 0.5 CH_2Cl_2: C 42.43, H 2.96, N 10.25; found: C 42.47, H 2.52, N 9.95. HR-MS (m/z): 311.5754, calculated for $[M–2PF_6]^{2+}$ 311.5685.

***κ*²-*C*,*N*-(*N*,*N''*-dimethyl-4-(2-pyridyl)-triazol-5-ylidene)bis(2,2'-bipyridine)ruthenium bis(triflate) (3e).** Complex **2e** (50 mg, 0.08 mmol), 2,2-bipyridine (25 mg, 0.16 mmol) and AgOTf (41 mg, 0.16 mmol) in DMSO (3 mL) were heated in a closed vial at 150 °C for 16 h. After cooling, CH_2Cl_2 (10 mL) and then Et_2O (60 mL) were added and vigorously shaken. The red oily precipitate was collected by decantation and precipitated twice from CH_2Cl_2/Et_2O, dried, and finally filtered as CH_2Cl_2

solution through celite. Solvent concentration and addition of pentane yielded **3e** d as a dark red solid (35 mg, 45%). ^{1}H NMR (CD_2Cl_2, 500 MHz): δ = 8.53 (d, 1H, $^{3}J_{HH}$ = 8.1 Hz, H^{3}_{bpy}), 8.45–8.40 (m, 3H, H^{3}_{bpy}), 8.27 (d, 1H, $^{3}J_{HH}$ = 5.4 Hz, H^{3}_{pyr}), 8.12–8.06 (m, 2H, H^{4}_{bpy}), 8.04 (td, 1H, $^{3}J_{HH}$ = 8.1 Hz, $^{4}J_{HH}$ =1.4 Hz, H^{4}_{bpy}), 7.97–7.92 (m, 3H, H^{4}_{bpy} + H^{4}_{pyr} + H^{6}_{bpy}), 7.77 (d, 1H, $^{3}J_{HH}$ = 5.7 Hz, H^{6}_{pyr}), 7.68, 7.62, 7.58 (3 × d, 1H, $^{3}J_{HH}$ = 5.7 Hz, H^{6}_{bpy}), 7.52–7.47 (m, 3H, H^{5}_{bpy}), 7.44 (ddd, 1H, $^{3}J_{HH}$ = 8.1 Hz, $^{3}J_{HH}$ = 5.7 Hz , $^{4}J_{HH}$ = 1.4 Hz, H^{5}_{bpy}), 7.16 (ddd, 1H, $^{3}J_{HH}$ = 8.1 Hz, $^{3}J_{HH}$ = 5.7 Hz , $^{4}J_{HH}$ = 1.4 Hz, H^{5}_{pyr}), 4.62, 3.69 (2 × s, 3H, NCH_3). $^{13}C\{^{1}H\}$ NMR (CD_2Cl_2, 125.5 MHz): δ 182.4 (C–Ru), 157.1, 156.5, 156.3 (C^{2}_{bpy}), 156.1 (C^{6}_{bpy}), 155.7 (C^{2}_{bpy}), 152.1 (C^{2}_{pyr}), 151.6, 151.5 (C^{6}_{bpy}), 151.2 (C^{6}_{bpy}), 149.1 (C^{6}_{pyr}), 146.0 (C_{trz}–pyr), 138.2, 137.9 (C^{4}_{bpy}), 137.1 (C^{4}_{pyr}), 136.9, 136.8 (C^{4}_{bpy}), 128.1, 127.9, 127.8 (C^{5}_{bpy}), 124.9 (C^{5}_{pyr}), 124.0, 123.9, 123.8, 123.7 (C^{3}_{bpy}), 121.6 (C^{3}_{pyr}), 39.0 (CH_3), 38.9 (CH_3). Elemental analysis calcd for $C_{31}H_{26}F_6N_8O_6RuS_2$ (885.8): C 42.03, H 2.96, N 12.65; found: C 41.85, H 2.45, N 12.61.

Complex 5. A mixture of complex **4** (90 mg, 0.12 mmol) and 2,2'-bipyridine (19 mg, 0.12 mmol) in DMSO (4 mL) was heated at 125 °C for 18 h. After cooling, CH_2Cl_2 (10 mL) and then Et_2O (60 mL) were added and vigorously shaken. The red oily precipitate was collected by decantation and washed twice by adding CH_2Cl_2 followed by Et_2O. The residue was washed with copious amounts of CH_2Cl_2 until the organic phase was colorless, thus affording **5** as a yellow solid (50 mg, 47%). An analytically pure sample was obtained from diffusion of Et_2O into a MeCN solution of **5**. ^{1}H NMR (CD_3CN, 500 MHz): δ 10.05 (d, 1H, $^{3}J_{HH}$ = 5.5 Hz, H_{bpy}), 8.62 (d, 1H, $^{3}J_{HH}$ = 8.3 Hz, H_{bpy}), 8.42–8.38 (m, 2H, H_{bpy}), 8.07 (td, 1H, $^{3}J_{HH}$ = 8.3 Hz, $^{4}J_{HH}$ = 1.2 Hz, H_{bpy}), 8.03–8.00 (m, 3H, H_{bpy} + H_{pyr}), 7.98 (d, 1H, $^{3}J_{HH}$ = 5.6 Hz, H_{bpy}), 7.41 (ddd, 1H, $^{3}J_{HH}$ = 8.3 Hz , $^{3}J_{HH}$ = 5.6 Hz , $^{4}J_{HH}$ = 1.2 Hz, H_{bpy}), 7.24–7.21 (m, 2H, H_{pyr}), 4.76, 4.56 (2 × s, 3H, NCH_3), 3.02, 2.70, 2.62, 2.45 (4 × s, 3H, $CH_{3\ DMSO}$). $^{13}C\{^{1}H\}$ NMR (CD_3CN, 125.5 MHz): δ 171.3 (C–Ru), 156.6 ($_{pyr}$), 156.0 (C_{bpy}), 155.7 (C_{bpy}), 155.6 (CH_{bpy}), 152.1 (CH_{pyr}), 150.3 (CH_{pyr}), 146.4 (C_{trz}–pyr), 141.5 (CH_{bpy}), 141.3 (CH_{pyr}), 141.0 (CH_{bpy}), 139.1 (CH_{bpy}), 129.2 (CH_{bpy}), 127.1 (CH_{bpy}), 126.5 (CH_{bpy}), 125.6 (CH_{bpy}), 123.4 (CH_{pyr}), 48.2, 46.3, 45.8, 41.5 (4 × $CH_{3\ DMSO}$), 41.4 (NCH_3),

40.5 (NCH_3). Elemental analysis calcd for $C_{25}H_{30}F_6N_6O_8RuS_4$ (885.9): C 33.90, H 3.41, N 9.49; found: C 33.51, H 3.37, N 9.31.

Crystallographic details: Crystal data for **2a** and **5** were collected using an Oxford Diffraction SuperNova A diffractometer fitted with an Atlas detector and using monochromated Mo–K_α radiation (0.71073 Å). An at least complete dataset was collected, assuming that the Friedel pairs are not equivalent. An analytical numeric absorption correction was performed[30] for both crystals as implemented in PLATON.[31] The structures were solved by direct methods using SHELXS-97[32] and refined by full matrix least-squares on F^2 for all data using SHELXL-97. Their isotropic thermal displacement parameters were fixed to 1.2 times (1.5 times for methyl groups) the equivalent one of the parent atom. Anisotropic thermal displacement parameters were used for all non-hydrogen atoms. Further crystallographic details are compiled in the supporting information. CCDC numbers 922584 (**2a**) and 922585 (**5**) contain the supplementary crystallographic data for this paper. These data can be obtained free of charge from the Cambridge Crystallographic Data Centre via www.ccdc.cam.ac.uk/data_request/cif.

Acknowledgements. We thank Dr. Nikitin (UCD) for support in molecular modeling. We gratefully acknowledge financial support by the European Research Council for a starting grant (ERC-StG 208561) and Science Foundation Ireland, and we thank Johnson Matthey for a generous loan of precious metals.

Supporting Information Available. UV-vis spectra for complexes **3a–e**, CV of **3c**, and X-ray crystal data for **2a** and **5** in CIF format. This material is available free of charge via the Internet at http://pubs.acs.org.

References

(1) (a) Hagfeldt, A.; Grätzel, M. *Chem. Rev.* **1995**, *95*, 49–68. (b) Hagfeldt, A.; Grätzel, M. *Acc. Chem. Res.* **2000**, *33*, 269. (c) Nazeerudin, M. K. *Coord. Chem. Rev.* **2004**, *248*, 1161–1164. (d) Grätzel, M. *Inorg. Chem.* **2005**, *44*, 6841–6851. (e) Ardo, S.; Meyer, G. J. *Chem. Soc. Rev.* **2009**, *38*, 115. (f) O'Regan, B. C.; Durrant, J. *Acc. Chem. Res.* **2009**, *42*, 1799–1808.

(2) See for example (a) Argazzi, R.; Murakami Iha, N. Y.; Zabri, H.; Odobel, F.; Bignozzi, C. A. *Coord. Chem. Rev.* **2004**, *248*, 1299–1316. (b) Campbell, W. M.; Burrell, A. K.; Officer, D. L.; Jolley, K. W. *Coord. Chem. Rev.* **2004**, *248*, 1363–1379. (c) Nogueira, A. F.; Longo, C.; De Paoli, M.-A. *Coord. Chem. Rev.* **2004**, *248*, 1455–1468. (d) Bredas, J.-L.; Durrant, J. R. *Acc. Chem. Res.* **2009**, *42*, 1689–1690 (special issue).

(3) (a) Slinker, J. D.; Gorodetsky, A. A.; Lowry, M. S.; Wang, J. J.; Parker, S.; Rohl, R.; Bernhard, S.; Malliaras, G. G. *J. Am. Chem. Soc.* **2004**, *126*, 2763–2767. (b) Lowry, M. S.; Goldsmith, J. I.; Slinker, J. D.; Rohl, R.; Pascal, R. A.; Malliaras, G. G.; Bernhard, S. *Chem. Mater.* **2005**, *17*, 5712–5719.

(4) (a) Bessho, T.; Constable, E. C.; Graetzel, M.; Hernandez Redondo, A.; Housecroft, C. E.; Kylberg, W.; Nazeeruddin, M. K.; Neuburger, M.; Schaffner, S. *Chem. Commun.* **2008**, 3717–3719. (b) Bozic-Webber, B.; Chaurin, V.; Constable, E. C.; Housecroft, C. E.; Meuwly, M.; Neuburger, M.; Rudd, J. A.; Schõnhofer, E.; Siegfried, L. *Dalton. Trans.* **2012**, *41*, 14157–14169. (c) Luo, S. P.; Mejía, E.; Friedrich, A.; Pazidis, A.; Junge, H.; Surkus, A. E.; Jackstell, R.; Denurra, S.; Gladiali, S.; Lochbrunner, S.; Beller, M. *Angew. Chem. Int. Ed.* **2013**, *52*, 419–423.

(5) (a) Islam, A.; Sugihara, H.; Hara, K.; Singh, L. P.; Katoh, R.; Yanagida, M.; Takahashi, Y.; Murata, S.; Arakawa, H.; Fujihashi, G. *Inorg. Chem.* **2001**, *40*, 5371–5380. (b) Geary, E. A. M.; Yellowlees, L. J.; Jack, L. A.; Oswald, I. D. H.; Parsons, S.; Hirata, N.; Durrant, J. R.; Robertson, N. *Inorg. Chem.* **2005**, *44*, 242–250.

(6) Ferrere, S.; Gregg, B. A. *J. Am. Chem. Soc.* **1998**, *120*, 843–844.

(7) Hasselmann, G. M.; Meyer, G. J. *J. Phys. Chem. B* **1999**, *103*, 7671–7675.

(8) Altobello, S.; Argazzi, R.; Caramori, S.; Contado, C.; Da Fre, S.; Rubino, P.; Chone, C.; Larramona, G.; Bignozzi, C. A. *J. Am. Chem. Soc.* **2005**, *127*, 15342–15343.

(9) For representative reviews, see: (a) Juris, A.; Balzani, V.; Barigelletti, F.; Campagna, S.; Belser, P.; von Zelewsky, A. *Coord. Chem. Rev.* **1988**, *84*, 85–277. (b) Purugganan, M. D.; Kumar, C. V.; Turro, N. J.; Barton, J. K. *Science* **1988**, *241*, 1645–1649. (c) Balzani, V.; Juris, A. *Coord. Chem. Rev.* **2001**, *211*, 97–115. (d) Spiccia, L.; Deacon, G. B.; Kepert, C. M. *Coord. Chem. Rev.* **2004**, *248*, 1329–1341. (e) Richter, M. M. *Chem. Rev.* **2004**, *104*, 3003–3036. (f) Constable, E. C. *Chem. Soc. Rev.* **2007**, *36*, 246–253. (g) Ward, M. D. *Chem. Commun.* **2009**, 4487–4499. (h) Youngblood, W. J.; Lee, S.-H. A.; Maeda, K.; Mallouk, T. E. *Acc. Chem. Res.* **2009**, *42*, 1966–1973. (i) McConnell, A. J.; Lim, M. H.; Olmon, E. D.; Song, H.; Dervan, E. E.; Barton, J. K. *Inorg. Chem.* **2012**, *51*, 12511–12520.

(10) (a) Grätzel, M. *Nature*. **2001**, *414*, 338–344. (b) Nazeeruddin, M. K.; Pechy, P.; Renouard, T.; Zakeeruddin, S. M.; Humphry-Baker, R.; Compte, P.; Liska, P.; Cevey, L.; Costa, E.; Shklover, V.; Spiccia, L.; Deacon, G. B.; Bignozzi, C. A.; Grätzel, M. *J. Am. Chem. Soc.* **2001**, *123*, 1613–1624. (c) Hagfeldt, A.; Boschloo, G.; Sun, L.; Kloo, L.; Pettersson, H.; *Chem. Rev.* **2010**, *110*, 6595–6663. (d) Yella, A.; Lee, H.-W.; Tsao, H. N.; Yi, C.; Chandiran, A. K.; Nazeeruddin, M. K.; Diau, E. W.-G.; Yeh, C.-Y.; Zakeeruddin, S. M.; Grätzel, M. *Science*, **2011**, *334*, 629–634.

(11) (a) Wadman, S. H.; Kroon, J. M.; Bakker, K.; Lutz, M.; Spek, A. L.; van Klink, G. P. M.; van Koten, G. *Chem. Commun.* **2007**, 1907–1909. (b) Wadman, S. H.; van Leeuwen, Y. M.; Havenith, R. W. A.; van Klink, G. P. M.; van Koten, G. *Organometallics* **2010**, *29*, 5635–5645.

(12) (a) Bourissou, D.; Guerret, O.; Gabbai, F. P.; Bertrand, G. *Chem. Rev.* **2000**, *100*, 39–92. (b) Hahn, F. E.; Jahnke, M. C. *Angew. Chem. Int. Ed.* **2008**, *47*, 3122–3172. (c) Arduengo, A. J.; Bertrand,

G. *Chem. Rev.* **2009**, *109*, 3209–3210. (d) Boydston A. J.; Bielawski, C. W. *Dalton Trans.* **2006**, 4073–4077. (e) Melaimi, M.; Soleilhavoup, M.; Bertrand, G. *Angew. Chem. Int. Ed.* **2010**, *49*, 8810–8849.

(13) (a) Albrecht, M. *Science*. **2009**, *326*, 532–533. (b) Schuster, O.; Yang, L.; Raubenheimer, H. G.; Albrecht, M. *Chem. Rev.* **2009**, *109*, 3445–3478. (c) Donnelly, K. F.; Petronilho, A.; Albrecht, M. *Chem. Commun.* **2013**, *49*, 1145–1159.

(14) Mercs, L.; Albrecht, M. *Chem. Soc. Rev.* **2010**, *39*, 1903–1912.

(15) For related approaches involving Arduengo-type carbenes, see: (a) Koizumi, T.; Tomon, T.; Tanaka, K. *Organometallics* **2003**, *22*, 970–975. (b) Kaufhold, O.; Hahn, F. E.; Pape, T.; Hepp, A. *J. Organomet. Chem.* **2008**, *693*, 3435–2440. (c) Chang, W.-C.; Chen, H.-S.; Li, T.-Y.; Hsu, N.-M.; Tingare, Y. S.; Li, C.-Y.; Liu, Y.-C.; Su, C.; Li, W.-R. *Angew. Chem. Int. Ed.* **2010**, *44*, 8161–8164. (d) Park, H.-J.; Kim, K. H.; Choi, S. Y.; Kim, H.-M.; Lee, W. I.; Kang, Y. K.; Chung, Y. K. *Inorg. Chem.* **2010**, *49*, 7340–7352. For approaches investigating triazole-derived carbenes, see: (e) Schulze, B.; Escudero, D.; Friebe, C.; Siebert, R.; Görls, H.; Köhn, U.; Altuntas, E.; Baumgaertel, A.; Hager, M. D.; Winter, A.; Dietzek, B.; Popp, J.; Gonzalez, L.; Schubert, U. S. *Chem. Eur. J.* **2011**, *17*, 5494–5498. (f) Brown, D. G.; Sanguantrakun, N.; Schulze, B.; Schubert, U. S.; Berlinguette, C. P. *J. Am. Chem. Soc.* **2012**, *134*, 12354–12357. (g) Brown, D. G.; Schauer, P. A.; Borau-Garcia, J.; Fancy, B. R.; Berlinguette, C. P. *J. Am. Chem. Soc.* **2013**, *135*, 1692–1695.

(16) (a) Nazeeruddin, M.K.; Rodicio, I.; Humphry-Baker, R.; Muller, E.; Liska, P.; Vlachopoulos, N.; Grätzel, M. *J. Am. Chem. Soc.* **1993**, *115*, 6382–6390. (b) Haque, S. A.; Palomares, E.; Cho, B. M.; Green, A. N. M.; Hirata, N.; Klug, D. R.; Durrant, J. R. *J. Am. Chem. Soc.* **2005**, *127*, 3456–3462.

(17) Ghattas, W.; Müller-Bunz, H.; Albrecht, M. *Organometallics,* **2010**, *29*, 6782–6789.

(18) (a) Wang, H. M. J.; Lin, I. J. B. *Organometallics* **1998**, *17,* 972–975. (b) Chianese, A. R.; Li, X.; Janzen, M. C.; Faller, J.W.; Crabtree, R.H. *Organometallics* **2003**, *22*, 1663–1667. (c) Garrison, J. C.;

Youngs, W. J. *Chem. Rev.* **2005**, *105,* 3978–4008.

(19) (a) Prades, A.; Viciano, M.; Sanaú, M.; Peris, E.; *Organometallics* **2008**, *27,* 4254–4259. (b) Gandolfi, C.; Heckernoth, M.; Neels, A.; Laurenczy, G.; Albrecht, M. *Organometallics*. **2009**, *28*, 5112–5121. (c) Bernet, L.; Lalrempuia, R.; Ghattas, W.; Mueller-Bunz, H.; Viagara, L.; Llobet, A.; Albrecht, M. *Chem. Commun.,* **2011**, 47, 8058–8060. (d) Mercs, L.; Neels, A.; Stoeckli-Evans, H.; Albrecht, M. *Inorg. Chem.* **2011**, *50*, 8188–8196.

(20) (a) Le Lagadec, R.; Rubio, L.; Alexandrova, L.; Toscano, R. A.; Ivanova, E. V.; Meskys, R.; Laurinavicius, V.; Pfeffer, M.; Ryabov, A. D. *J. Organomet. Chem.* **2004**, *689,* 4820–4832. (b) Kuang, D.; Ito, S.; Wenger, B.; Klein, C.; Moser, J.-E.; Humphry-Baker, R.; Zakeeruddin, S. M.; Grätzel, M. *J. Am. Chem. Soc.* **2006**, *128,* 4146–4154. (c) Chen, H.-S.; Chang, W.-C.; Su, C.; Li, T.-Y.; Hsu, N.-M.; Tingare, Y. S.; Li, C.-Y.; Shie, J.-H.; Li, W.-R. *Dalton Trans.* **2011**, *40*, 6765–6770.

(21) Rillema, D. P.; Jones, D. S. *J. Chem. Soc., Chem. Commun.,* **1979**, 848–849.

(22) Mathew, P.; Neels, A.; Albrecht, M. *J. Am. Chem. Soc.* **2008**, *130*, 13534–13535. (b) Terashima, T.; Inomata, S.; Ogata, K.; Fukuzawa, S.-i. *Eur. J. Inorg. Chem.* **2012**, 1387–1393. (c) Yuan, D.; Huynh, H. V. *Organometallics* **2012**, *31*, 405–412.

(23) For similar lifetimes of benzimidazoles, see: O'Reilly, E. J.; Dennany, L.; Griffith, D.; Moser, F.; Keyes, T. E.; Forster, R. J. *Phys. Chem. Chem. Phys.* **2011**, *13*, 7095–7101.

(24) Cao, F.; Oskam, G.; Meyer, G. J.; Searson, P. C. *J. Phys. Chem.* **1996**, *100*, 17021–17027.

(25) Lever, A. B. P.; *Inorg. Chem.* **1990**, *29*, 1271–1285.

(26) Bredas, J.L.; Norton, J.E.; Cornol, J. Coropceanu, V. *Acc. Chem. Res.* **2009**, *42*, 1691–1699.

(27) (a) Catalano, V. J.; Etogo, A. O. *J. Organomet. Chem.* **2005**, *690*, 6041–6050. (b) Chianese, A. R.; Brener, P. T.; Wong, C.; Reyes, R. J. *Organometallics* **2009**, *28*, 5244–5252. (c) Starikova, O.V.;

Dolgushin, G.V.; Larina, L.I.; Ushakov, P.E.; Komarova, T.N. *Russ. J. Org. Chem.* **2003**, *39*, 1467–1470. (d) Grundemann, S.; Albrecht, M.; Kovacevic, A.; Faller, J. W.; Crabtree, R. H. *J. Chem. Soc., Dalton Trans*. **2002**, 2163–2167.

(28) Connelly, N. G.; Geiger, W. E. *Chem. Rev*. **1996**, *96*, 877–910.

(29) Creaven, B .S.; George, M. W.; Ginzburg, A. G.; Hughes, C.; Kelly, J. M.; Long, C.; McGrath, I. M.; Pryce, M. T. *Organometallics* **1993**, *12*, 3127–3131.

(30) Clark, R. C.; Reid, J. S. *Acta Cryst*. **1995**, *A51*, 887–897.

(31) Spek, A. L. *J. Appl. Cryst*. **2003**, *36*, 7–13.

(32) Sheldrick, G. M. *Acta Cryst*. **2008**, *A64*, 112–122.

Figure for TOC